Chiral Solvent Structure around Chiral Molecules: Experimental and Theoretical Study

Julie Fidler,† P. Mark Rodger,*,† and Alison Rodger‡

Contribution from the Department of Chemistry, University of Reading, Whiteknights, P.O. Box 224, Reading, RG6 2AD, U.K., and Physical Chemistry Laboratory, South Parks Road, Oxford, OX1 3QZ, U.K.

Received February 9, 1994. Revised Manuscript Received May 5, 1994•

Abstract: Molecular dynamics simulations of bromocamphor in *n*-hexane, CCl_4, and $CHCl_3$ were performed at three temperatures to establish the distribution of the solvent molecules about the solute and to see how this changed with temperature. The results were used to calculate the solvent contribution to the circular dichroism (CD) of the solute at each temperature. The variation in experimental CD as a function of temperature was also measured for bromocamphor, dibromocamphor, camphor, and fenchone in *n*-hexane, CCl_4, and $CHCl_3$. Since the intrinsic CD of the solute is essentially temperature independent, the variation in measured CD as a function of temperature could be attributed solely to the solvent-induced CD. The results of calculations and experiments were used to explain the chiral solvent distribution induced about itself by a chiral molecule. The observed effects were able to be explained in terms of pockets around the solute being occupied by the solvent and therefore creating a dissymmetric arrangement around the optically active carbonyl chromophore. This effect was found to be very temperature dependent. The magnitude of the solvent effect was found to depend upon the nature of the solute as well as the solvent.

1. Introduction

The role of a solvent, and particularly its local configuration around solute molecules, in biology and enantiomeric selectivity is something that has attracted intermittent interest in the past. However, there seems to be growing speculation that local solvent structuring may actually be intrinsic to the mechanism by which certain biological processes occur. An extreme example of this can be found in the way the water-structuring properties of glycopeptides are utilized as an antifreeze agent in the blood of arctic fish, but other examples in which a role for solvent structuring has been postulated include taste quality and sweetness-perception,[1,2] and drug lifetimes *in vivo*.[3]

Solvents are known to influence chiral properties. For example the circular dichroism (CD) of carbonyl n–π^* transitions in rigid molecules is affected by the choice of solvent to the extent that the sign of the CD signal may change between different achiral solvents.[4-8] In some instances this is due to a change in the conformers found in solution. However, Moscowitz *et al.*[4] observed similar changes in rigid systems where there was no conformational equilibrium for the solute, and they explained their observations in terms of a solvation equilibrium, where the equilibrium was between "solvated" and "unsolvated" molecules. The term "solvated molecule" was taken to mean a solute molecule implicitly bound to a solvent, and the "unsolvated molecule" was therefore unbound. Kirk *et al.*[5] went further in their analysis of solvent effects on CD and proposed that "the solvent effect is due to a dissymmetric arrangement of associated solvent molecules in relation to the carbonyl. The CD due to the carbonyl compound itself is assumed to be constant and subject to an increment depending upon the nature and the degree of the dissymmetry of the associated solvent". Even though it has been realized that solvation effects can be largely due to the local configuration of the solvent, there is still a lack of detailed information on the shape and nature of the solvation shell around a solute.

In this report, molecular dynamics (MD) simulations have been combined with experimental CD spectroscopy in an attempt to probe the solvent structure around a chiral molecule. Previously,[9] we showed that spherical achiral solvents may contribute as much as 20% of the calculated CD intensity of certain camphors; this was found to be due to the camphors inducing a chiral collective-structure in the solvent even though the solvent molecules themselves are achiral. The present objective is to use a more realistic model for the solvent and compare the MD results directly with experimental data. The MD simulations were used to characterize the distribution of the solvent about the solute and therefore establish the chirality of the solvation shell. The magnitude of the observable effect of the solvation shell on the CD could then be calculated from this distribution for the comparison with experiment. CD spectroscopy was used as the experimental probe to quantify the chirality of the solvent distribution. In this paper we present MD simulations of (+)-3-bromocamphor dissolved in the solvents *n*-hexane, CCl_4, and $CHCl_3$; we note that, unlike the 9,10-dibromocamphor considered in our earlier work.[9] (+)-3-bromocamphor has only one significant conformation, and so solvent-induced changes in the CD spectrum of the solute will be related to solvent structuring rather than solvent-induced conformational changes. The choice of solvent has been made to accommodate both experimental and modeling considerations: all three solvents are commonly used in spectroscopic studies and reliable, well-tested intermolecular potentials are available for them. At the same time they provide a good extension of our earlier, rather simplified, study which concentrated on solvent/solute interactions arising between methyl/camphor or CCl_4/camphor groups. $CHCl_3$ also provides a comparable study with a polar solvent.

CD spectra were measured for (+)-camphor (**1**), (+)-3-bromocamphor (**2**), 9,10-(+)-dibromocamphor (**3**), and (–)-fenchone (**4**), in each of the solvents *n*-hexane, CCl_4, and $CHCl_3$

* Author to whom correspondence should be addressed.
† University of Reading.
‡ Physical Chemistry Laboratory.
• Abstract published in *Advance ACS Abstracts,* June 15, 1994.
(1) Shamil, S.; Birch, G. G.; Mathlouthi, M.; Clifford, M. N. *Chem. Senses* **1987**, *12*, 397.
(2) Birch, G. G.; Shamil, S. *J. Chem. Soc., Faraday Trans.* **1988**, *84*, 2635.
(3) Bangham, A. D. *Biol. Cell* **1983**, *47*, 1.
(4) Moscowitz, A.; Wellman, K. M.; Djerassi, C. *Proc. Natl. Acad. Sci. U.S.A.* **1963**, *50*, 799.
(5) Kirk, D. N.; Klyne, W.; Wallis, S. R. *J. Chem. Soc. C* **1970**, 350.
(6) Lightner, D. A.; Eng, F. P. C. *Steroids* **1980**, *35*, 189.
(7) Lightner, D. A.; Bouman, T. D.; Wijekoon, W. M. D.; Hansen, A. E. *J. Am. Chem. Soc.* **1986**, *108*, 4484.
(8) Rodger, A.; Rodger, P. M. *J. Am. Chem. Soc.* **1988**, *110*, 2361.
(9) Fidler, J.; Rodger, P. M.; Rodger, A. *J. Chem. Soc., Perkin Trans. 2* **1992**, 235.

0002-7863/94/1516-7266$04.50/0

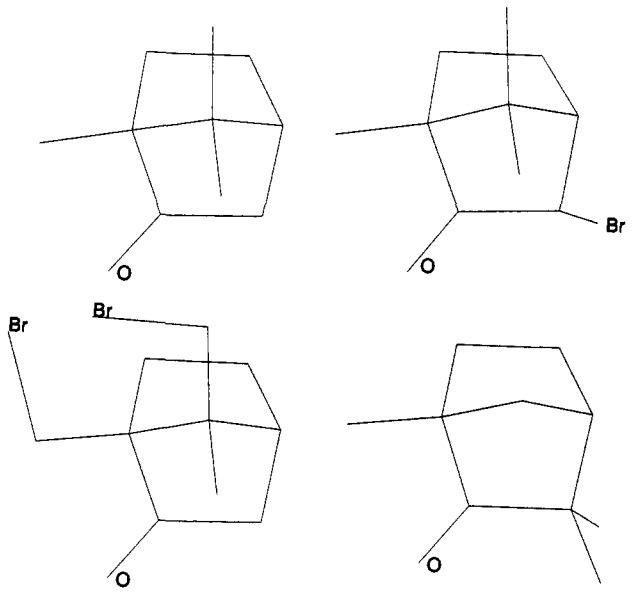

Figure 1. From left to right and top to bottom, **1**, **2**, **3**, and **4**.

as a function of temperature (see Figure 1). This enabled a comparison across series of both solutes and solvents. In the absence of conformational changes of the solute, any temperature dependence of the CD intensity can be attributed directly to the solvent as the CD intensity is inherently temperature independent.

A brief summary of the theory of the CD of the n–π^* transition of carbonyls is given in the next section. This is followed by the details of the simulations and calculations of the solvent-induced CD, along with the experimental methods. The results we obtained are then presented with a detailed discussion and interpretation.

2. CD of the n–π^* Transition of the Carbonyl

To be able to compare experiment and theory, a physical quantity has to be determined from both experiment and theory under comparable conditions. In CD, this quantity is the rotatory strength, R, which can be determined experimentally from the intensity of the CD spectra as a function of wavelength and can also be calculated theoretically, and so we have a means of linking CD spectra with calculated values of R.

The mechanism giving rise to the rotatory strength of the n–π^* transition of the carbonyl group in the camphors is well understood.[10] To a first approximation, the carbonyl itself is achiral and the CD arises as a result of perturbation by its asymmetric environment, this is known as the independent systems/perturbation approach. For a more detailed description see refs 11, 12, and 13. The rotatory strength induced in a C_{2v} carbonyl chromophore can be written

$$R_{n-\pi^*} = \sum_c (T_1 + T_2 + T_3) \quad (1)$$

where

$$T_1 = r_c^{-3} K_{mom}^{ch}[qxy] \quad (2)$$

$$T_2 = r_c^{-4} K_{mom}^{dip}[\mu_x y(1 - 5x^2) + \mu_y x(1 - 5y^2) + 5\mu_z(xyz)] \quad (3)$$

(10) Kirk, D. N. *Tetrahedron* **1986**, *42*, 777.
(11) Moffit, W.; Woodward, R. B.; Moscowitz, A.; Klyne, W.; Djerassi, C. *J. Am. Chem. Soc.* **1961**, *83*, 4013.
(12) Höhn, E. G.; Weigang, O. E. *J. Am. Chem. Soc.* **1968**, *48*, 1127.
(13) Schipper, P. E.; Rodger, A. *Chem. Phys.* **1986**, *109*, 173 and references therein. Schipper, P. E.; Rodger, A. *Chem. Phys.* **1985**, *98*, 29.

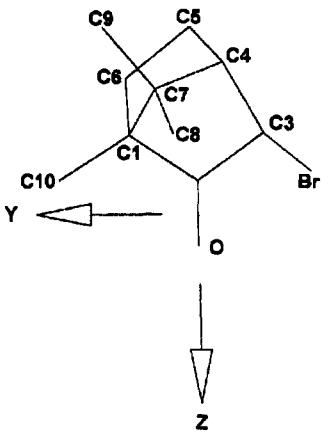

Figure 2. Coordinate system and numbering of carbons used within this work for bromocamphor. The x-axis points out of the page to produce a right-handed system.

$$T_3 = r_c^{-4} 12 K_{mom}^{pol}[5\alpha_{zz}xyz + \alpha_{zx}y(5x^2 - 1) + \alpha_{zy}x(5y^2 - 1)] \quad (4)$$

and the summation is over all chromophores C of the system excluding the carbonyl group. K_{mom} is a transferable constant for the carbonyl which depends on the transition moments involved and the mechanism by which the CD is induced and is related to the Franck–Condon factor; q is the charge on C; μ_u, $u = (x,y,z)$, are the components of the permanent electric dipole on C; α_{zu} is the zu component of the polarizability of C; r_c is the distance between the C origin and that of the carbonyl; and (x,y,z) are the components of the unit vector along the line from the origin of the carbonyl to that of C in the coordinate system defined by Figure 2.

In this study the chromophores C were taken to be the atoms or functional groups within the solvent, while the contribution from the rest of the solute is ignored; for rigid molecules, such as the camphor derivatives considered here, the latter will be essentially constant and so cannot lead to any temperature dependence.

If there are no strongly polar or charged groups present, then T_3 is the dominant contribution to $R_{n-\pi^*}$. If charged groups are present, then T_1 must be included. Previously,[9] we used nonpolar, uncharged, spherical solvents and so considered only the isotropic polarizability term in T_3, *i.e.* the α_{zz} term; however, given the more realistic model of the solvent in the present work, the anisotropic terms, α_{zx} and α_{zy}, also have to be included. In our model of $CHCl_3$ we have represented its dipole by partial charges on the atoms in the molecule, and so the charge term T_1 was also calculated for this solvent.

3. Methods

Simulation Method. Algorithm. The algorithm used for the MD simulation in this work is similar to that described previously.[9] Several minor differences were required due to the intramolecular motion of the solvent: in particular a time step of 2 fs was used (instead of 5 fs) to keep the energy fluctuations within 0.01% of NkT in constant energy/constant volume simulations; also simulations were performed on a Silicon Graphics Indigo workstation. The systems were allowed to equilibrate for 10 ps, whereupon a further 800 ps was simulated, taking about 60 h of CPU time on a SG R4000 Indigo. This was obtained by performing 20 successive simulations of 40 ps, starting from the equilibrated configuration. All 20 simulations were then statistically averaged.

Potentials. United atom Lennard–Jones potentials, as developed by Jorgensen,[7] were used for the solute. This resulted in a 12-site model for bromocamphor. The potentials used for the

Table 1. Lennard–Jones Parameters for Atoms and Groups

	Solute				
parameter	C(sp^3)	C(sp^2)	H	O	Br
ϵ/k, K	81.0	81.0	0.0	80.0	161.0
σ, Å	3.91	3.91		2.85	3.88

	Solvents						
	hexane		CCl_4		$CHCl_3$		
parameter	CH_3	CH_2	C	Cl	C	Cl	H
ϵ/k, K	88.06	59.38	51.2	102.4	51.2	150.73	9.996
σ, Å	3.90	3.90	3.2	3.5	3.4	3.44	2.2
q, e					0.179	−0.087	0.082

Table 2. Bond Polarizabilities Used for the Calculation of $R_{n-\pi^*}$

bond	$\alpha_\parallel{}^a/(10^{-40}$ C m^2 V$^{-1})$	$\alpha_\perp{}^a/(10^{-40}$ C m^2 V$^{-1})$
C—H	0.77	0.70
C—C	1.00	0.33
C—Cl	4.22	2.10

[a] $\parallel$ and $\perp$ to the bond axis.

solvents were chosen to enable them to mimic structural features of the solvent molecules and are as follows (see Table 1): *n*-hexane was described by a six-site united atom model which treated the CH_2 and CH_3 groups as single spherical sites;[14] CCl_4 was described by treating each atom explicitly using LJ potentials;[15] $CHCl_3$ was also described by treating all five atoms explicitly, again using LJ potentials but this time supplemented with partial charges on each atom, giving a molecular dipole of 1.1 D.[16] The potentials for both solute and solvent are summarized in Table 1. All solvent models reproduced the corresponding experimental values for the internal configuration energy at 298 K and 1 atm.

Calculation of Solvent-Induced CD. *n*-Hexane and CCl_4 are both nonpolar and uncharged, so eq 4 was used to calculate R. Molecular polarizabilities were described in terms of bond polarizabilities, and the requisite values are given in Table 2.[17] Both polarizability and electrostatic perturbation must be considered in $CHCl_3$. Polarizability effects were modeled as for the *n*-hexane and CCl_4, taking polarizable bonds to be the perturbing chromophores and using eq 4. For the electrostatic term we note that within the simulations the molecular dipole of $CHCl_3$ was described in terms of partial atomic charges; it therefore makes sense to consider the individual solvent atoms as the perturbing chromophores for the electrostatic interaction, in which case the additional contribution to the solvent-induced CD is described by eq 2.

In addition to the total solvent-induced CD, the radial dependence of R was calculated by averaging the R contribution over all the solvent molecules found in a thin shell of radius r that is centered on the C=O bond. This gave a measure of how different regions of the solvent contribute to the overall CD and will be called the radial CD intensity (RCD).

Chiral Solvent Structure. To examine the chiral solvent structure, we developed a method of analysis which can evaluate the asymmetric distribution of the solvent using the point symmetry projections of the C_{2v} point group.[9] The unperturbed carbonyl has C_{2v} symmetry, and it is known that the solvent adopts the symmetry of the solute,[18] so any deviation from a C_{2v} solvent distribution represents the effect of the rest of the solute molecule. The distribution of the solvent can then be separated into symmetry-adapted radial distribution functions (SARDF); four projections were defined: g_{A1}, g_{A2}, g_{B1}, and g_{B2}, where each element is projected following the irreducible representations of the C_{2v} character table. The SARDFs were calculated by adding and subtracting the densities in each xy quadrant in a manner specified by the character table. The two SARDFs of most interest are g_{A1}, which represents the totally symmetric (normal) RDF, and g_{A2}, which shows the breakup of symmetry associated with the zx and zy reflection planes and is the only chiral projection under C_{2v} symmetry. To aid us even further in our analysis, both SARDF and RCD were separated into contributions from the positive z and negative z regions. This enabled us to look at the solvent structure in the $+z$ and $-z$ hemispheres, allowing a more thorough examination. Note that the bulk of the solute molecule lies in the $-z$ hemisphere, while the $+z$ hemisphere contains just solvent and the solute carbonyl oxygen.

Table 3. Calculated Solvent Contributions to the Carbonyl n–π^* CD of 3-Bromocamphor

	$R^*/10^{-9}$ [a]	
temp, K	CCl_4	$CHCl_3$
263	4.15 ± 0.64	89 ± 32
293	3.85 ± 0.55	−108 ± 33
323	0.04 ± 0.69	−81 ± 35

[a] R^* is the reduced rotatory strength, defined in eq 5.

Circular Dichroism Spectroscopy. The CD spectra were measured on a JASCO J720 spectropolarimeter with the following conditions: response time was 0.5 s; eight scans were accumulated; the spectra were smoothed using a Fourier transform routine, taking care to ensure that structure was not lost or created from noise in the process.

The combination of four solutes and three solvents gave us 12 systems to study. The CD spectra of each system was measured at five temperatures: 10, 20, 30, 40, and 50 °C. Any solvent effect on the CD was probed by taking the highest temperature spectrum as our "zero" spectrum (this was closest to the gas-phase CD due to there being less association with the solvent as the appropriate boiling temperature is reached; the boiling temperatures are 69 °C for *n*-hexane, 62 °C for CCl_4, and 77 °C for $CHCl_3$) and subtracting it from the other temperatures to give a "difference" spectrum. Since the CD intensity of these rigid solutes is temperature independent, any difference observed could be attributed solely to chiral solvent structure.

The experimental rotatory strengths were calculated using the frequency-weighted area under the CD curve,[19] which could then be compared with the rotatory strengths calculated from the distribution of the solvent obtained from the simulations.

Materials. The four solutes—**1**, **2**, **3**, and **4**, see Figure 1—were all obtained from Aldrich supplies, AR grade, and used without further purification. The three solvents were all of spectroscopic grade.

4. Results

Computer Simulation of 3-Bromocamphor. *n*-Hexane. The total solvent-induced CD vanished (within the statistical uncertainty of the calculations) at each temperature considered. Figure 3 shows an example of the g_{A1}, g_{A2}, and RCD in the $+z$ and $-z$ hemispheres at 293 K; it is clear that there is substantial cancellation of the positive and negative signals, resulting in no net contribution to the CD from the solvent.

Simulations at the other two temperatures showed similar behavior. From these results it was predicted that *n*-hexane would not make an observable effect on the CD.

(14) Mcdonald, I. R.; Bounds, D. G.; Klein, M. L. *Mol. Phys.* **1982**, *45*, 521.
(15) Jorgensen, W. L.; Madura, J. D.; Swenson, C. J. *J. Am. Chem. Soc.* **1984**, *106*, 6638.
(16) Dietz, W.; Heinzinger, K. *Ber. Bunsen-Ges Phys. Chem.* **1985**, *89*, 968.
(17) Allen, G. W.; Aroney, M. J. *J. Chem. Soc., Faraday Trans. 2* **1989**, *85*, 247.
(18) Whiffin, D. H. *Mol. Phys.* **1988**, *63*, 1053.
(19) Moffit, W.; Moscowitz, A. *J. Chem. Phys.* **1959**, *30*, 648.

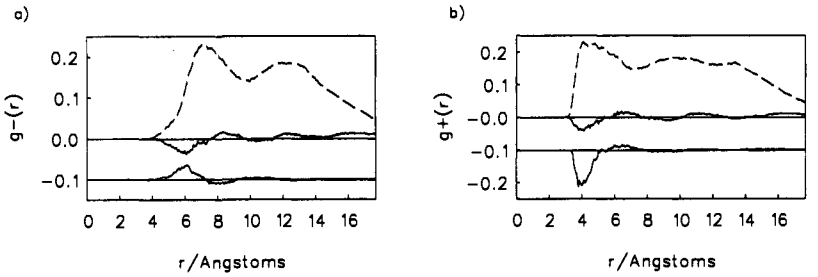

Figure 3. SARDF (g_{A1} (- -) and g_{A2} (—) upper) and the RCD ((—) lower) for bromocamphor in *n*-hexane at 293 K in (a) the $-z$ hemisphere and (b) the $+z$ hemisphere. The RCD has been shifted down by 0.1 and multiplied by a constant factor for clarity.

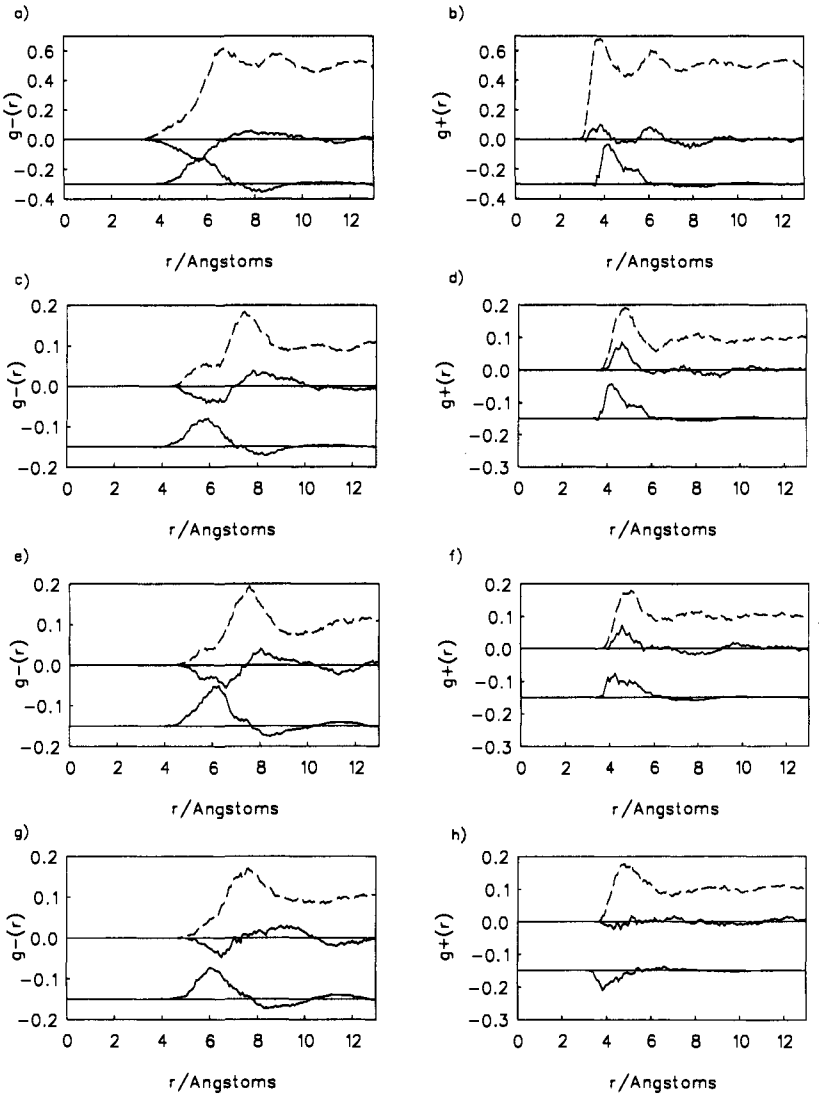

Figure 4. SARDF (g_{A1} (- -) and g_{A2} (—) upper) and the RCD ((—) lower) for bromocamphor in CCl_4, which has been split up into contributions from the chlorine atoms (a and b) and the carbon atoms (c–h) in (a) the $-z$ hemisphere at 263 K; (b) the $+z$ hemisphere at 263 K; (c) the $-z$ hemisphere at 263 K; (d) the $+z$ hemisphere at 263 K; (e) the $-z$ hemisphere at 293 K; (f) the $+z$ hemisphere at 293 K; (g) the $-z$ hemisphere at 323 K; (h) the $+z$ hemisphere at 323 K. The RCD has been shifted down by 0.3 for chlorine and 0.15 for carbon and multiplied by a constant factor for clarity.

CCl_4. The calculated total solvent-induced CD is given in Table 3 in terms of reduced rotatory strengths, R^*:

$$R^* = R_{n-\pi^*}/12K_{mom} \quad (5)$$

The uncertainties quoted are the standard deviations obtained from each set of 20 × 40 ps simulation. At the 95% confidence limit, the R^* values at 263 and 293 K are both significantly larger than zero, but R^* at 323 K is not. This suggests that there is a trend for less solvent structure at the higher temperatures. In Figure 4 g_{A1} and g_{A2} are separated into contributions from the two different atom types, *i.e.* the carbons and the chlorines, but the RCD is the total contribution. Both the carbon and the chlorine atoms produced curves which showed the same variations when the temperature was raised. For this reason, the contribution from the chlorines is shown at one temperature only.

The RDFs for the carbons and the chlorines are consistent with the intramolecular structure of the solvent molecules: the carbon is surrounded by chlorines so should be further away from the carbonyl. This is seen in the way the g_{A1} peak starts earlier for chlorine than carbon. The g_{A2} peak for carbon is positioned between the two peaks for chlorine, which again reflects the shape of the CCl_4 molecule. In all cases the first solvation shell is

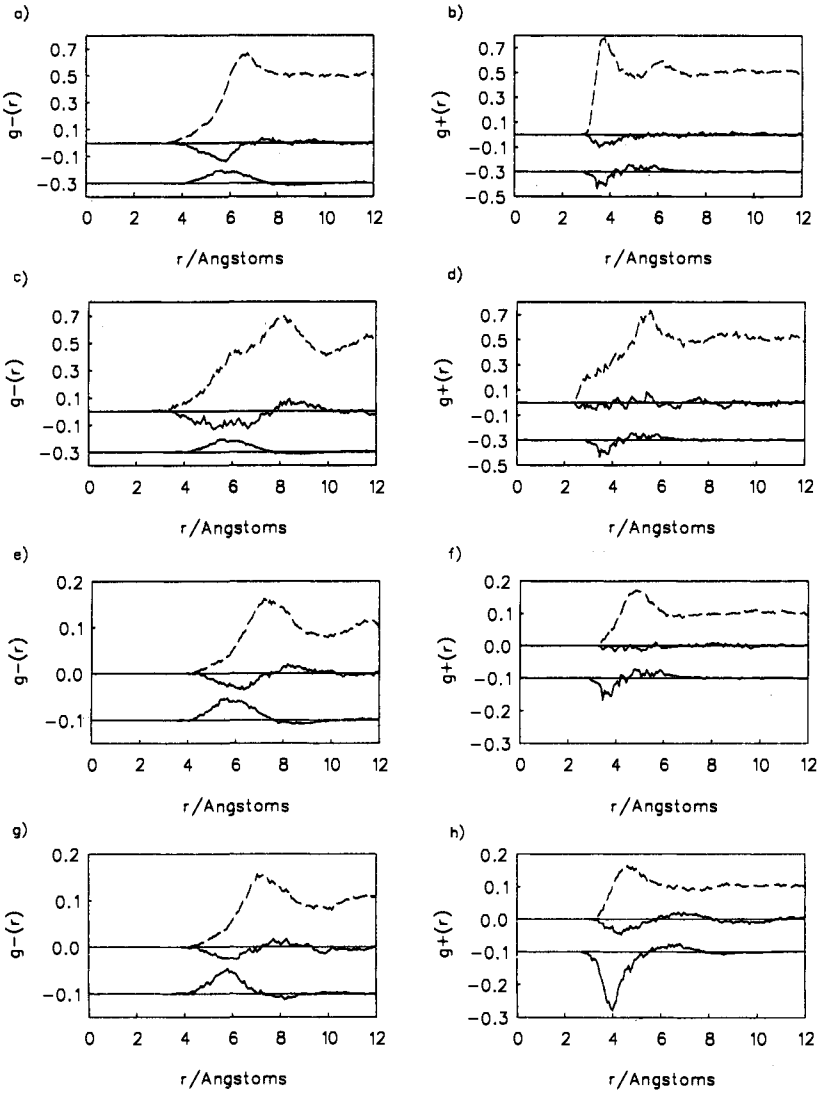

Figure 5. SARDF (g_{A1} (- -) and g_{A2} (—) upper) and the RCD ((—) lower) for bromocamphor in $CHCl_3$, which has been split into contributions from the chlorine atoms (a and b), the hydrogen atoms (c and d), and the carbon atoms (e–h) in (a) the $-z$ hemisphere at 263 K; (b) the $+z$ hemisphere at 263 K; (c) the $-z$ hemisphere at 263 K; (d) the $+z$ hemisphere at 263 K; (e) the $-z$ hemisphere at 263 K; (f) the $+z$ hemisphere at 263 K; (g) the $-z$ hemisphere at 293 K; (h) the $+z$ hemisphere at 293 K. The RCD has been shifted down by 0.3 for chlorine and hydrogen and 0.1 for carbon and multiplied by a constant factor for clarity.

well-defined, and there is evidence of a second solvation shell from g_{A1}, but the chiral structure appears to extend only to the first solvation shell with g_{A2}, showing no structure beyond 8 Å.

The most striking feature of these plots is in the $+z$ hemisphere, where the RCD actually changes sign with increasing temperature: from a positive to a negative CD. A change in sign of the CD is a very substantial effect to observe and is made more interesting by the fact that it is seen in the $+z$ hemisphere; the solute is located in the $-z$ hemisphere, and so we did not expect to see a strong chiral solvent effect in the $+z$ hemisphere. The structure in the $-z$ hemisphere does not appear to change with temperature with all the curves being very similar.

$CHCl_3$. In prineiple $CHCl_3$ has two contributions to the CD, a charge contribution and a polarization contribution; however, our calculations indicated that the charge contribution vanished at all three temperatures, and so only the polarization term is discussed; these values are given in Table 3. At the 95% confidence limit all three values are significantly different from zero. Statistical analysis revealed no significant difference between values at 323 and 293 K, so these are taken to be the same; however, the 263 K R^* is significantly different. Indeed a change in the sign of the total solvent-induced CD is observed: from positive to negative as the temperature is raised. Figure 5 shows g_{A1}, g_{A2}, and RCD for various combinations of hemisphere and atom type (C, H, and Cl).

Again the g_{A1} peaks correlate well with the molecular structure of the solvent; the first peak for C lies in between the first two peaks for both Cl and H. The very low concentration of H close to the solute suggests that the solvent molecules are preferentially aligning with the H atoms pointing away from the solute's carbonyl group. In the $+z$ hemisphere, g_{A2} at 263 K shows no chiral structure for C and H and very little for Cl; however, at 293 K there is quite a substantial chiral structure. This is the reverse of the behavior that would be expected from simple solute–solvent association arguments and opposite to that which we observed with CCl_4. In other words, our results for the $CHCl_3$ solvent indicate an increase in solvent-induced CD with increasing temperature. As with CCl_4, we see no change in the $-z$ hemisphere, but a dramatic change in the $+z$ hemisphere. The trend in the $+z$ hemisphere is actually the same as for CCl_4; the RCD peak gets more negative.

CD Spectroscopy. Camphor. The spectra of camphor in all solvents showed no net solvent contribution to the CD. The "difference" spectra showed pronounced vibrational structure,

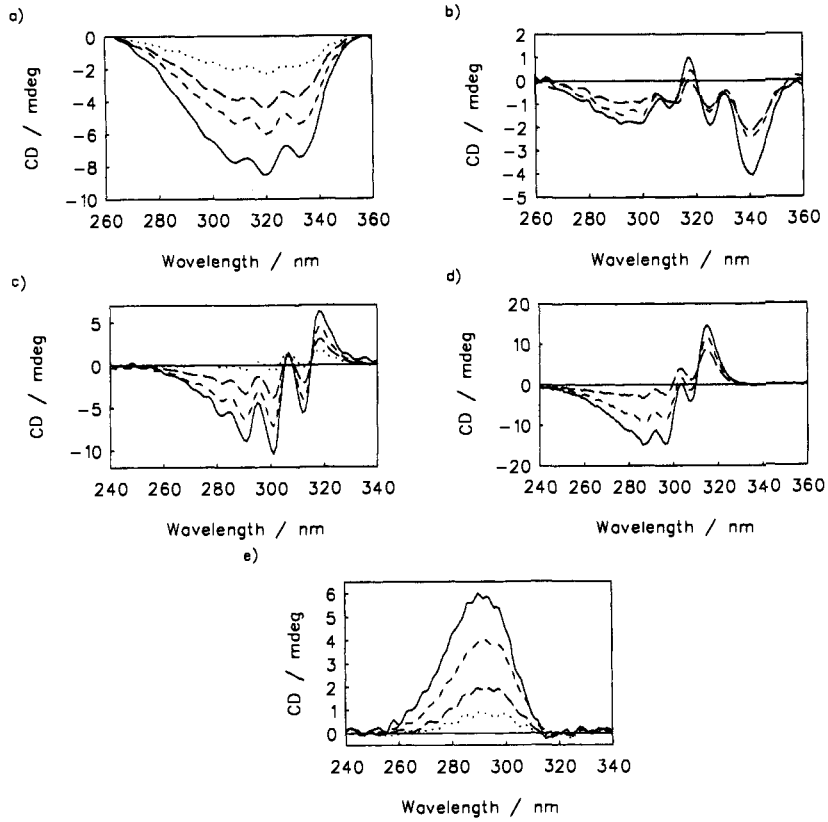

Figure 6. Difference CD spectra for (a) bromocamphor in $CHCl_3$; (b) bromocamphor in CCl_4; (c) dibromocamphor in *n*-hexane; (d) dibromocamphor in CCl_4; (e) fenchone in $CHCl_3$. The temperature differences are (in °C) 50–10 (—), 50–20 (- - -), 50–30 (– –), and 50–40 (···).

but the total CD intensities, defined by

$$R = \int \frac{I(\lambda)}{\lambda} d\lambda$$

were not significantly different from zero, hence implying that intensity was simply shifting between the vibronic bands.

Bromocamphor. In *n*-hexane there is pronounced vibrational structure in the difference spectra, which is again due to intensity shift between the vibronic bands, and again there is no net solvent effect on the total intensity. In $CHCl_3$ (Figure 6a) and CCl_4 (Figure 6b), a medium-sized change in the magnitude of the area under the curves was observed with changing temperature differences. CCl_4 showed a slightly smaller effect than $CHCl_3$, which could be due to the dipole in $CHCl_3$ aligning with the carbonyl and so enhancing structure in the solvation shell.

Dibromocamphor. In *n*-hexane (Figure 6c), the difference spectra again show an intensity shift between the vibronic bands, but in this case there was also a net change in the CD intensity. The net contribution, though very small, was larger than that for any other solute in *n*-hexane. The difference spectra in CCl_4 (Figure 6d) and $CHCl_3$ were very similar. Again, vibronic intensity shift is seen, but there is also a large difference in the areas under the curves for the various temperature differences, indicating a significant solvent effect. The magnitudes of these solvent effects were greater than those observed with any of the other camphor derivatives considered.

Fenchone. All the solvents behaved similarly to $CHCl_3$, which is shown in Figure 6e. The solvent-induced CD in CCl_4 was of the same magnitude as in $CHCl_3$, but in *n*-hexane it was much smaller and rendered the solvent effect insignificant. *n*-Hexane also showed more vibrational structure than $CHCl_3$.

5. Discussion

There was a good agreement between theory and experiment for all three solvents modeled.

The simulations of bromocamphor in *n*-hexane showed no solvent dependence or temperature dependence. This behavior is in accord with experiment, as the spectra also showed no temperature dependence; as explained in section 3, any temperature dependence in the CD intensity of rigid molecules must arise from solvent dependent perturbations, and so the absence of any significant temperature dependence was taken to imply no solvent dependence in the CD.

The simulations of bromocamphor in CCl_4 did show a solvent dependence at and below 293 K. This behavior agreed with the spectra where a significant temperature and hence solvent dependence was observed. From the experimental data it was seen that the intrinsic CD of the bromocamphor is negative, and from the calculations, R^* is positive at all temperatures (Table 3). From this it can be inferred that the solvent-induced CD is diminishing the intrinsic CD of the solute, and this diminishing effect is smaller at higher temperatures due to the loss of chirality in the solvent structure.

The SARDF and RCD curves (Figure 4) from the simulations show that the change in CD can be attributed to the solvent structure in the $+z$ hemisphere at a distance between 3 and 6 Å from the origin of the carbonyl; this is the region where the RCD changes sign. To understand more completely what happens to the solvent structure in that region as temperature increases, we used the simulations to calculate the full angular distribution of the solvent about the bromocamphor. This resulted in a density distribution plot for the $+z$ hemisphere (*i.e.* in spherical polar coordinates: $\theta \in [0,\pi/2]$; $\phi \in [0,2\pi]$) between 3 and 6 Å. This enabled us to examine whether the solvent dependence arose from thermal expansion of the solvent, from restructuring within the solvation shell (with solvent moving from positive to negative octants), or from a combination of the two to give anisotropic expansion. Thermal expansion always accompanies an increase in temperature and was observed in the simulations by an increase in volume at higher temperatures. However, this expansion was too small to account for the change in CD. Figure 7 shows the

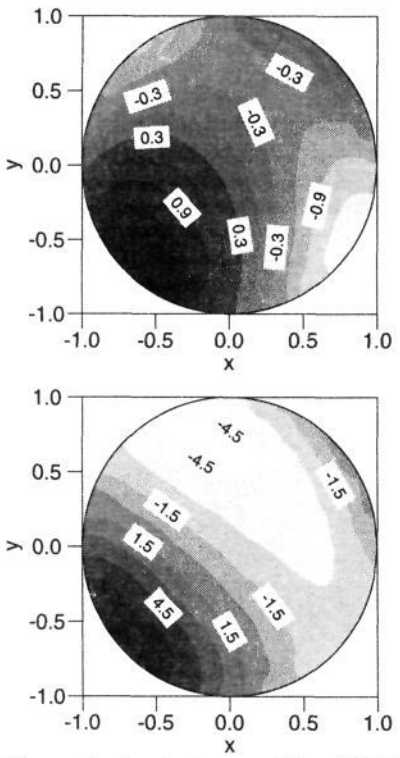

Figure 7. Difference-density plots between 293 and 323 K in CCl_4, for the $+z$ hemisphere, describing a shell between 3.75 and 4.25 Å from the carbonyl. A positive density represents a lower density at the higher temperature, *i.e* solvent moves away from that region on heating; negative density represents movement toward that region on heating. Shown at the top is carbon density, at the bottom, chlorine density. x and y are the angular part of the spherical polar coordinates: $x = \sin\theta\cos\phi$; $y = \sin\theta\sin\phi$, where θ and ϕ are the polar and azimuthal angle, respectively.

difference-density plots between 293 and 323 K for CCl_4 in the $+z$ hemisphere, *i.e.* the density at 323 K subtracted from the density at 293 K. Note that of the carbon and chlorine atoms it is the former that are more easily identified with the molecular centers and hence which identify shifts in solvent density most clearly. In the carbon difference-density it is observed that there is a specific movement away from the $--+$ (xyz) octant, which results in the loss of a positive contribution to the CD. There is a corresponding gain of density in the $+-+$ octant but it is not large enough in area to account for the movement of all the atoms from the $--+$ octant, so we conclude that most of the solvent was redistributed evenly over the rest of the solvation shell. Also note that any density on or near the axes will give no or very little contribution to the solvent-induced CD, so the negative chlorine difference-density of –4.5 can mostly be ignored. The question is then can we identify the reason for this migration?

In the bromocamphor molecule there are two possible "pockets" where a solvent molecule can sit. One is made by C8, C9, and C10 (pocket 1), and the other is made by C5, C6, and Br (pocket 2). QUANTA CHARMm (developed by Molecular Simulations Inc.) was used to observe visually how the solvent molecules would lie in these "pockets". This was achieved by taking one solute molecule and one solvent molecule and placing the solvent molecule near the pocket. The energy of the configuration was then minimized, and the resultant configuration was examined. Care had to be taken to ensure that the solvent neither left the pocket during minimization nor was caught in a local, rather than global, minimum. The procedure was repeated for both pockets. The resulting minimized energies (using CHARMm parameters) were 127 and 124 kJ mol^{-1} for pocket 1 and pocket 2, respectively. The difference between the energies is approximately kT, which corresponds to the thermal energy and, within the uncertainty of the CHARMm potential parameters, is negligible. In pocket 1, three Cl atoms of the solvent are anchored onto the pocket, with the fourth Cl pointing away. They are anchored in such a way that they are staggered with respect to the pocket. This is a very compact arrangement and so will be favored by the packing considerations that dominate liquid structure. The position of the solvent molecule is in the $++-$ octant, thus giving the negative RCD at 8 Å from the origin. The sign of the RCD at approximately 8 Å did not change with temperature, which suggests the CCl_4 on average remains anchored in the same way throughout the temperature change. Pocket 2 only enabled one Cl to point into the pocket with the other three Cl pointing away and slightly downward into the $-x$ region. This packing is less compact compared with that of pocket 1, and so the solvent molecule has more vibrational freedom. The position of the solvent is in the $--+$ octant, thus giving a positive contribution to the RCD at 4 Å in the $+z$ hemisphere. As the temperature was increased, this peak in the RCD changed sign, which corresponds to movement of that solvent molecule away from pocket 2 at high temperatures. This also corresponds to the movement of solvent density from the $--+$ octant observed in the angular distribution plots (Figure 7). The net effect of the solvent-induced CD is still positive, as it is dominated by the $-z$ hemisphere, but the magnitude gets smaller with increasing temperature since there is this change of handedness in the $+z$ hemisphere associated with the structural changes around pocket 2.

It may be asked why the two pockets behave so differently when their minimized energies are so similar. The minimized energy calculations are for an isolated dimer, whereas the MD and CD data are for the condensed liquid. In the condensed phase there are many other solvent molecules competing for the little free volume that is available, and so free energy considerations will tend to favor more efficient packing of molecules. Thus, pocket 2, where the lowest potential energy is associated with a more spacious solute–solvent association, will give a less stable arrangement of the solvent than pocket 1. It is pocket 2, therefore, that allows more solvent mobility and less solvent structure at higher temperatures.

$CHCl_3$ is slightly anomalous in that the calculated R^* gets increasingly negative with increasing temperature, thus implying an increase in solvent chirality (the intrinsic solute CD is negative) in contrast to one's expectations based on increased solvent mobility with temperature. However, the calculations do agree with experiment. The sign of the intrinsic CD for bromocamphor is negative, the calculated R^* is positive at 263 K and negative at and above 293 K, and the experiments do show a more negative rotatory strength at higher temperatures. From this combination of simulation and experiment we infer that the solvent-induced CD is diminishing the solute's intrinsic CD at low temperatures and enhancing it at the higher temperatures.

Again, the region of interest is 4 Å from the origin in the $+z$ region (Figure 5), but this time we have increasing chirality with temperature. Angular density distribution plots (Figure 8) show that between 263 and 293 K we have a specific movement of solvent from the $--+$ octant to the $-++$ octant. This would correspond to the loss of a positive contribution and the gain of a negative contribution to the CD, which is seen in the total R^* values (Table 3). Again we can explain these observations in terms of pockets around the solute and with the aid of QUANTA CHARMm. Pocket 1 and pocket 2 are as before, but in the $+z$ hemisphere we must now consider an additional pocket, that made by C6, C10, and O (pocket 3); this new pocket is too small to accommodate a Cl, but is large enough for a H. The minimized energies of pocket 2 and pocket 3 are 124 and 125 kJ mol^{-1}, respectively. The difference is again less than kT so is negligible. In pocket 3 the H and a Cl sit astride C10 and O with the H pointing in the direction of the pocket. This involves an interaction

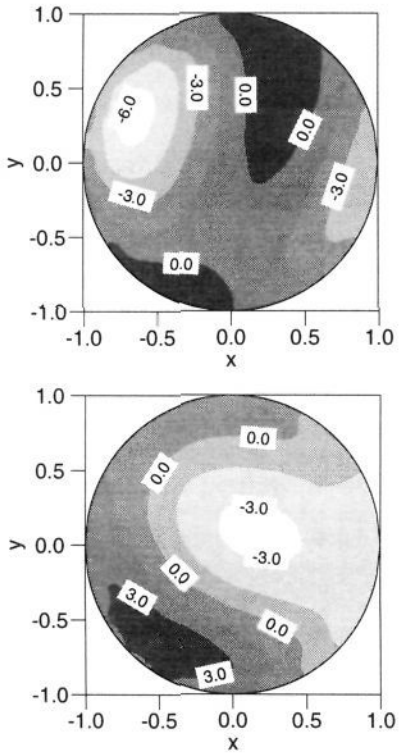

Figure 8. Difference-density plots between 263 and 293 K in $CHCl_3$, for the $+z$ hemisphere, describing a shell between 3.75 and 4.25 Å from the carbonyl (see caption to Figure 7).

between two atoms of the solvent so is a more compact type of packing compared with pocket 2 (but less than pocket 1). Pocket 3 is in the $- + +$ octant, so at low temperatures it will cancel out the positive contribution from pocket 2 and therefore gives no chirality. As the temperature is increased, the solvent leaves pocket 2 but remains in pocket 3, thus giving a more negative CD in the $+z$ hemisphere and rendering the total CD negative.

From the spectra we can obtain a lot of information about the nature of the solutes and the solvents. Looking across the series of solvents, it was seen that *n*-hexane did not make any significant contribution to the CD with any solute except dibromocamphor. This is not surprising when it is realized that *n*-hexane has always been considered by spectroscopists to be a nonassociative solvent, as evidenced by the high degree of vibrational structure retained in the solute spectra; a strong association with the solvent provides more paths for vibrational relaxation and therefore gives a weaker vibrational structure. CCl_4 and $CHCl_3$ both show solvent effects of approximately the same magnitudes for the same solute, though $CHCl_3$ shows a slightly larger effect due to its dipole, which will tend to align with the carbonyl, leading to a more structured solvent. This is also supported by the shift of λ_{max} to shorter wavelength in $CHCl_3$, which is in accord with the solvent dipole stabilizing the ground state. Such dipolar alignment may also be enhanced by accommodating the H in pocket 3, as identified from the simulations. Looking across the series of solutes, it is apparent that camphor cannot induce a chiral structure in any of the solvents, whereas dibromocamphor can induce a chiral structure in all the solvents, including *n*-hexane. Bromocamphor's and fenchone's ability to induce chiral solvent structures is intermediate, with bromocamphor slightly stronger than fenchone. The behavior across this series tends to suggest that bromines have a greater inducing power than the methyl groups with respect to solvent structure.

6. Conclusion

We have presented a full study into the local configuration of simple achiral solvents around a chiral solute and the effect of the solvation shell on the CD. We have achieved good agreement between theory and experiment. A simple interpretation of the data has been possible in terms of "pockets" created by the solute: these are sites where solute–solvent association can occur in a manner that optimizes solute–solvent packing effects.

It has been clearly established that the local configuration of the solvent does have a considerable effect on the CD of the solute and that by occupying pockets at low temperatures and vacating some at high temperatures, this contribution will generate temperature variations in the CD intensity. This will have important implications for asymmetric synthesis where certain reaction paths would be blocked by solvent molecules packed well into specific sites around the reactants. For a full understanding of solvent effects on enantioselectivity and molecular recognition, the local configuration and its effects must be established.

The experimental data show that the magnitude of the solvent effect depends strongly on the nature of the solute as well as the solvent, as some solutes are stronger in inducing chiral solvent structures than others.

Acknowledgment. The computational work was supported uncer SERC grant GR/H07207, A.R. acknowledges the support of the Glasstone Trust and J.F. the support of SERC and Reading University for a studentship and scholarship, respectively.